JOURNAL OF CATALYSIS **179,** 241–257 (1998)
ARTICLE NO. CA982194

Reaction and Surface Characterization Study of Higher Alcohol Synthesis Catalysts

IX. Pd- and Alkali-Promoted Zn/Cr-Based Spinels Containing Excess ZnO

David M. Minahan,* William S. Epling,† and Gar B. Hoflund†,[1]

*Union Carbide Corporation, Technical Center/P.O. Box 8361, South Charleston, West Virginia 25303; and †Department of Chemical Engineering, University of Florida, Gainesville, Florida 32611

Received March 2, 1998; revised June 11, 1998; accepted June 22, 1998

A Zn/Cr spinel support material was prepared which contains excess ZnO and then was promoted with 5.9 wt% Pd and varying amounts ranging from 0 to 7 wt% of either K or Cs. Each of these catalysts was tested at four different reactor operating conditions (T of 400 or 440°C and P of 1000 or 1500 psig) for higher alcohol synthesis (HAS) using a syngas feedstream (1 : 1 $CO : H_2$) after reductive pretreatment. High isobutanol production rates in conjunction with low methanol-to-isobutanol mole ratios ($\leq$1.0) and low hydrocarbon byproduct rates are desired. For the K-promoted catalysts the highest isobutanol production rates are obtained at the higher pressure and temperature settings of 1500 psig and 440°C, and methanol-to-isobutanol mole ratios below the ideal value of 1.0, which is required for downstream methyl tertiary-butyl ether (MTBE) synthesis, are obtained. The Cs-promoted catalysts generally yield higher isobutanol production rates than the K-promoted catalysts. The highest isobutanol production rate of 170 g/kg-h is obtained using the 3 wt% Cs-promoted catalyst at 1000 psig and 440°C. The lower pressure is economically advantageous with regard to process costs. Most importantly, this isobutanol production rate is quite high compared to others presented in the literature and demonstrates that Pd does enhance the synthesis of isobutanol. The catalytic activity remained stable over a 5-day test period for each catalyst. X-ray photoelectron spectroscopy (XPS) and ion scattering spectroscopy (ISS) were used to characterize these catalysts. The results obtained from these techniques indicate that pretreating the catalysts in 1×10^{-7} Torr of H_2 at 300°C for 4 h causes an enrichment of the near-surface alkali-promotor concentration. A layered structure forms which consists of this enriched alkali layer and an enriched Pd and ZnO layer which reside above the Zn/Cr spinel support material. The reaction process decreases the thickness of the alkali and ZnO layers and seems to trap the Pd in a thin layer above the support material but below the alkali promotors which reside at the surface. The surface areas of these catalysts are about 80 m^2/g, and they are stable with aging. The primary role of the Zn/Cr spinel is to provide a high surface-area support for the promoted ZnO.

INTRODUCTION

The addition of certain oxygenates to automobile fuel results in an increased octane number and, hence, more complete combustion and a reduction in hydrocarbon emissions. Due to heightened environmental concerns and the possibility of dwindling fuel supplies, research in this area has been considerable. Methyl tertiary-butyl ether (MTBE) is a common oxygenated additive found in gasoline used today and is typically added in quantities of 3–5 wt%. MTBE is derived from methanol and isobutylene precursors, and the isobutylene is produced from petroleum (C_4) feedstock. In order to reduce this dependence on the petroleum feed, a design utilizing a coal-derived, syngas feedstream (CO and H_2) to produce an equimolar mixture of isobutanol and methanol has been intensely studied. This equimolar mixture of alcohols can be processed downstream, through known technology (1) to form MTBE. The ideal methanol-to-isobutanol mole ratio of 1.0 is difficult to achieve, and values lower than 1.0 are preferred over higher values because methanol can more easily be added from other sources.

Three different types of higher alcohol synthesis (HAS) catalysts have received the most attention (2). These include modified Fischer–Tropsch catalysts alkali-modified, low-temperature, low-pressure methanol synthesis catalysts and alkali-modified, high-temperature, high-pressure methanol synthesis catalysts. A new class of HAS catalysts, based on the use of rare earth oxides, has also been studied (3,4). However, these catalysts produce very little isobutanol compared to the alkali-promoted, methanol synthesis catalysts and therefore result in very high methanol-to-isobutanol mole ratios. Of these HAS catalyst types, the alkali modified, high-temperature, high-pressure, methanol synthesis catalysts (Zn/Cr based) yield the lowest methanol-to-isobutanol mole ratios. Nevertheless, the other two catalyst groups have received more attention due to the less severe reaction conditions required.

---

[1] Corresponding author.

0021-9517/98 $25.00

This present study is part of a series (5–9) with the goal of optimizing the catalytic performance of the Zn/Cr spinel catalysts. Some of the catalysts described in this paper perform better than any other catalysts described in the literature to date. This optimization process is based on increasing the total alcohol and isobutanol production rates, increasing the product selectivity toward alcohols rather than hydrocarbons, and attaining methanol-to-isobutanol product mole ratios equal to or less than 1.0. The first of these studies included the testing and characterization of K- and Cs-promoted, commercially available, Zn/Cr spinel methanol synthesis catalysts (5,6). Surface characterization data obtained from these samples indicate that the near-surface regions of these catalysts consist primarily of ZnO, although the alkali promotors are bound to the Cr. No distinct spinel features are observed except when using X-ray diffraction, which is a bulk characterization technique. Subsequent studies sought to improve the catalyst performance and elucidate the active phase of HAS over these catalysts through the testing of a K-promoted ZnO powder (containing no Cr or spinel structure) (7) and K- and Cs-promoted, 1 : 1 and 3 : 1 (excess ZnO) Zn : Cr-based spinel catalysts (8). The nonpromoted ZnO powder does not result in HAS, but isobutanol production does occur when the ZnO powder is promoted with K. This result indicates that an alkali-promoted ZnO surface is the active catalytic phase for HAS. The 1 : 1 Zn : Cr spinel catalysts are also quite active, but, according to XPS data, a substantial amount of ZnO and a small amount of Zr/Cr spinel are present in the near-surface region of these samples, making it difficult to determine the active phase of this catalyst type. However, the addition of excess amounts of ZnO to these samples during the preparation results in significant improvements in the isobutanol production rate (8). Apparently, the spinel structure only functions as a high surface area support for the catalytically active, alkali-promoted ZnO. Forzatti *et al.* (1) and Simard *et al.* (10) have suggested that the acidity due to surface Cr is responsible for high hydrocarbon production rates. However, the hydrocarbon production rates also are quite large for K-promoted ZnO (7).

In a previous study by Keim and Falter (11), a Pd-containing catalyst was tested and found to be quite active toward HAS. Therefore, the effects of the addition of Pd to the Cs-promoted, 1 : 1 Zn : Cr catalysts on the reactor product stream composition have been examined in this series of studies (9). The addition of the Pd significantly enhances both the total alcohol production rate and the isobutanol production rate. Due to the beneficial effects of Pd and excess amounts of ZnO, another series of catalysts has been prepared and tested in this present study. These catalytic materials are Zn/Cr spinel based but prepared with excess amounts of ZnO and promoted with both 5.9 wt% Pd and varying amounts of K or Cs in order to determine the optimum alkali loadings. Vedage *et al.* (12) have demonstrated that the addition of Cs is superior to K for HAS using Cu/ZnO-based catalysts. More recent studies have been performed using K as the promotor (13–16), and since each catalyst system may inherently differ, the effects of both K and Cs addition on the product stream composition were examined in this present study. The preferred reactor operating parameters were determined by testing each of the catalysts, including a nonpromoted sample at two different operating reactor temperatures, 400 and 440°C, and two different pressures, 1000 and 1500 psig. These settings span the narrow range over which these HAS catalysts operate. At lower temperatures methanol is primarily produced, and above 450°C significant quantities of hydrocarbon by-products are formed, lowering the selectivity to alcohols. Appreciable catalytic activity occurs above 1000 psig, and the upper pressure limit was set at 1500 psig due to reactor limitations. For many of the catalysts tested, higher pressures probably would enhance performance, but process costs become uneconomical. X-ray photoelectron spectroscopy (XPS) and ion scattering spectroscopy (ISS) were used to characterize the samples in order to gain information about the composition and chemical species present in the near-surface region. These characterization results have led to identification of the active catalytic phase, demonstrate that the spinel structure is unimportant with regard to catalytic activity, provide compositional and chemical-state information, and provide information about how the surfaces change during pretreatment and aging. Further improvements in HAS catalyst performance will be based on the characterization results.

EXPERIMENTAL

The Zn/Cr spinel support material was prepared in a manner described previously (8), and the Zn/Cr ratio used in this study was 3 : 1. The support material was calcined in air for 12 h at 325°C and then promoted with Pd and K or Cs, using the incipient wetness method with Pd nitrate and the appropriate alkali nitrate precursors. After the addition of the promotors, the remaining product was dried at 100°C overnight. The catalyst powders were then inserted into the reactor and pretreated in a 5 vol% H_2 and N_2 mixture for 4 h at 325°C. The resulting catalysts all have BET surface areas of approximately 80 m^2/g which do not change with 5 days of aging. The reactor design and the system used to analyze the product stream have been described previously also (5). Briefly, the reactor consists of a Cu-lined tube, instead of the standard stainless steel tubing, to avoid side reactions with the tube walls. Tests were conducted which proved that no reactions at the tube walls occur under the conditions used in these studies. One gram of catalyst mixed with 3 volumes of glass beads was used in each reactor experiment, and each catalyst was tested for 5 days in the reactor in order to ensure catalyst stability. No significant changes in the product stream compositions were noted with time. The catalysts were tested under four sets of reactor conditions, two temperatures, 400 and 440°C, and two pressures, 1000 and 1500 psig. The feedstream consisted of a 1 : 1 CO : H_2 mixture which was purified using an activated carbon trap. The product stream was analyzed using a Varian 3700 gas chromatograph.

The experimental system used in the characterization studies has been described previously as well (5). XPS and ISS were used to analyze the near-surface region and the outermost atomic layer, respectively. The ISS parameters were set in order to minimize sample damage caused by ion sputtering. The as-prepared samples were inserted into an ultrahigh vacuum (UHV) system, characterized and then given a reductive treatment at 300°C for 4 h in 1×10^{-7} Torr of hydrogen. The samples were again characterized using XPS and ISS. Catalyst samples which were removed from the reactor after the 5-day test period were also characterized using XPS, ISS, and depth profiling, in order to observe changes in the surface chemistry caused by the reaction process.

RESULTS AND DISCUSSION

Reaction Studies

A comparison of the reactor product stream composition using a nonpromoted Zn/Cr catalyst containing excess ZnO and this same material promoted with 5.9 wt% Pd at the four different reactor settings is presented in Table 1. Since ZnO powder does not catalyze the production of isobutanol from syngas unless an alkali promotor has been added (7), the synthesis of isobutanol using the nonpromoted and Pd-promoted Zn/Cr catalysts without alkali addition may seem surprising, but small amounts of Na or K impurities are always present at these surfaces, which promote the production of small amounts of isobutanol. Characterization data presented below substantiate this claim. Larger alcohol production rates are obtained using these catalysts at the lower temperature of 400°C, while at 440°C greater hydrocarbon by-product rates are obtained. The largest amount of isobutanol produced using the Pd-promoted Zn/Cr catalyst without added alkali is a mere 18 g/kg-h. However, significant quantities of hydrocarbon by-products are formed over both of these materials, resulting in poor selectivities. The total hydrocarbon rates are provided in the tables, but the detailed hydrocarbon product distributions are not shown. They typically consist of about 50 mol% methane, 30 mol% ethane, 11 mol% propanes, 9 mol% butanes, and only trace quantities of high molecular weight hydrocarbons. Furthermore, the addition of Pd causes a decrease in the single-pass conversion rate. The addition of Pd to the nonalkali-promoted support material is not advantageous for HAS. An interesting result is the increase in the total alcohol production rate using the Pd-promoted catalyst at the higher temperature of 440°C, but lower pressure of 1000 psig versus 1500 psig. This increase and a corresponding large decrease in the hydrocarbon byproduct rate from 271 to 140 g/kg-h results in an increase in the alcohol selectivity from 25 to 47%. A similar trend was not observed in a previous part of this series regarding the effects of Pd addition to a 1 : 1 Zn : Cr spinel catalyst (9).

TABLE 1

Product Stream Composition Using a Zn/Cr Spinel with Excess ZnO and Promoted with

	0 wt% Pd				5.9 wt% Pd			
P(psig)	1000	1500	1500	1000	1000	1500	1500	1000
T(°C)	400	400	440	440	400	400	440	440
Selectivity to total alcohols (%)	50	61	29	29	37	50	25	47
Total alcohol rate (g/kg-h)	164	292	170	118	137	278	172	247
Methanol rate (g/kg-h)	160	285	154	101	129	243	152	243
Ethanol rate (g/kg-h)	0	0	0	0	0	0	0	0
Isopropanol rate (g/kg-h)	0	0	4	2	0	0	0	0
n-Propanol rate (g/kg-h)	0	1	5	6	0	0	6	0
Isobutanol rate (g/kg-h)	2	6	7	8	7	18	12	0
MeOH/i-ButOH mole ratio	185	110	51	29	43	31	29	—
Hydrocarbon rate (g/kg-h)	82	91	216	150	118	142	271	140
Conversion (%)	17	20	21	18	14	15	16	15

The effects of K addition to the 5.9 wt% Pd/Zn/Cr catalyst containing excess ZnO on the product stream composition at the four different reactor settings is shown in Table 2. The effects of K addition (as well as Cs) to the excess ZnO-containing Zn/Cr catalyst which does not contain Pd has been published previously (8). According to Table 2, both lower hydrocarbon by-product rates and isobutanol production rates are attained at 1000 psig and 400°C. At the higher pressure setting, the total alcohol production rate is increased in each case, as is the production rate of isobutanol. The drawback to the higher pressure at 400°C is the larger amounts of hydrocarbon by-products which are formed, but the selectivity to total alcohols is increased under these conditions due to the greater increase in the total alcohol formation rate. Operating the reactor at the higher temperature of 440°C and a pressure of 1500 psig results in similar trends, slightly higher production rates of isobutanol and much larger hydrocarbon by-product rates, resulting in smaller total alcohol production rates. The higher hydrocarbon by-product rates contribute to the decrease in the total alcohol production rates, since less methanol is produced, because more of the reactants are converted to hydrocarbons. This results in a decrease in the selectivity to desired products at higher K loadings while at

TABLE 2

Product Stream Composition Using a 5.9 wt% Pd/Zn/Cr Spinel Containing Excess ZnO and Promoted with

	1 wt% K				3 wt% K				5 wt% K				7 wt% K			
P(psig)	1000	1500	1500	1000	1000	1500	1500	1000	1000	1500	1500	1000	1000	1500	1500	1000
T(°C)	400	400	440	440	400	400	440	440	400	400	440	440	400	400	440	440
Selectivity to total alcohols (%)	44	59	35	26	70	77	57	55	86	87	73	85	91	91	78	80
Total alcohol rate (g/kg-h)	113	264	210	96	159	294	221	136	137	240	190	161	171	313	239	158
Methanol rate (g/kg-h)	76	184	95	47	73	155	54	24	54	129	41	48	76	180	53	21
Ethanol rate (g/kg-h)	1	3	16	0	1	4	8	8	0	0	0	0	0	2	3	0
Isopropanol rate (g/kg-h)	0	0	0	0	1	1	5	6	0	0	0	1	3	3	10	5
n-Propanol rate (g/kg-h)	2	6	20	12	4	12	18	14	9	17	15	9	24	36	42	47
Isobutanol rate (g/kg-h)	34	72	77	36	81	121	136	84	74	94	134	102	69	93	132	85
MeOH/i-ButOH mole ratio	5.2	5.9	2.9	3.0	2.1	3.0	0.92	0.66	1.7	3.2	0.71	1.1	2.5	4.5	0.93	0.57
Hydrocarbon rate (g/kg-h)	81	102	235	166	43	51	111	78	14	21	50	20	11	18	45	29
Conversion (%)	12	16	18	13	17	21	23	18	12	15	17	15	14	15	15	16

the lower K loadings of 1 and 3 wt%, the lowest selectivity to total alcohols occurs at 1000 psig and 440°C due to significant drops in the amount of alcohols formed at the lower pressure and a smaller decrease in the amount of hydrocarbons formed. Except in the case of the 7 wt% K-promoted catalyst, the largest single-pass conversions are obtained at 440°C and 1500 psig. The methanol-to-isobutanol mole ratios are lower at the higher temperature due to the increased amounts of isobutanol formed. Ratios near the ideal value of 1.0 are actually obtained at 440°C and 1500 psig using the 3, 5, and 7 wt% K-promoted catalysts.

For the K-promoted catalysts, the most isobutanol is formed at 440°C and 1500 psig. The effects of K loading on the total alcohol rate is plotted in Fig. 1a for these operating parameters. The Pd-supported Zn/Cr spinel results in the lowest alcohol production rates. The addition of 1 wt% K to this catalyst increases the total alcohol production rate to 210 g/kg-h, and the addition of 3 wt% K increases this value to 221 g/kg-h. These increases are due to substantial gains in the isobutanol production rates as shown in Fig. 1b with 136 g/kg-h of isobutanol produced using the 3 wt% K-promoted catalyst. These values are substantially greater than values previously reported in the literature for K-promoted, Cu/ZnO-based HAS catalysts (12,17) and about 32% higher than that obtained from a commercially available methanol synthesis catalyst promoted with K (5). Although decreases in the methanol production rates are observed, the greater enhancement of isobutanol production rates results in increased total alcohol production rates. The addition of 5 wt% K to the Pd-promoted Zn/Cr material results in a decrease in both the isobutanol and methanol production rates resulting in the decrease in the total alcohol production rate shown in Fig. 1a. The total alcohol production rate increases with the addition of 7 wt% K, but this increase is due to the greater amount of methanol formed over this catalyst. The effect of K addition on the selectivity to total alcohols at 440°C and 1500 psig is shown in Fig. 2a. The Pd-promoted Zn/Cr catalyst is only 25% selective to alcohols at these conditions. The addition of 1 wt% K results in an increase

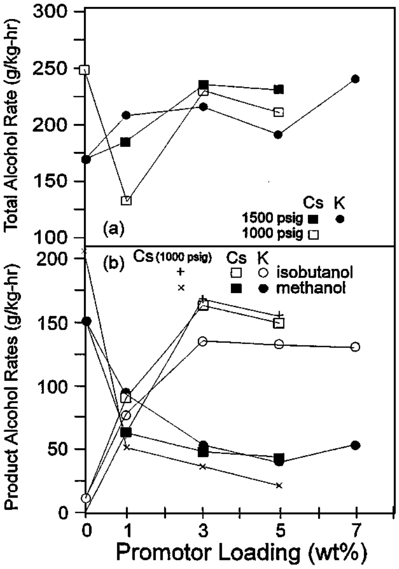

FIG. 1. The effect of K and Cs loading on (a) the total alcohol production rate and (b) the isobutanol and methanol production rates at 440°C and either 1000 or 1500 psig.

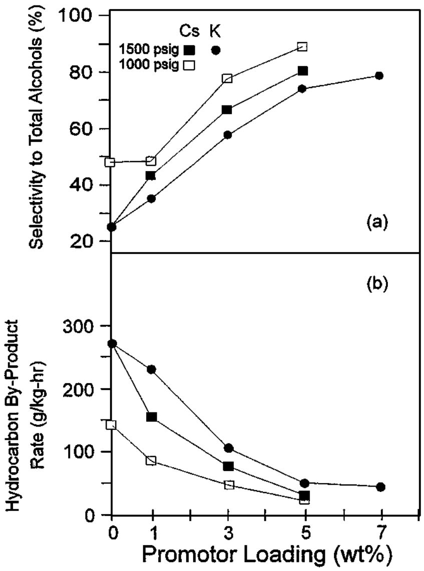

FIG. 2. The effect of K and Cs loading on (a) the selectivity to total alcohols (calculated on a molar and CO_2- and H_2O-free basis) and (b) the total hydrocarbon production rate at 440°C and either 1000 or 1500 psig.

in the selectivity to 35%, and increasing amounts of K promotor causes further increases in the selectivity. However, the rate of selectivity increase decreases at 7 wt% K. This increase in the selectivity to total alcohols is mirrored by a decrease in hydrocarbon by-product rates, as shown in Fig. 2b. With each increase in the amount of K promotor, the hydrocarbon by-product rate decreases. Again the rate of decrease, much like the rate of increase in the selectivity, slows with the addition of 7 wt% K. Similar trends in the hydrocarbon by-product rates and selectivities have been observed previously (5–9). Simard *et al.* (10) have demonstrated that the highest yields of hydrocarbons occur over Zn/Cr-based catalysts when the amount of Zn is minimized, i.e. the amount of surface Cr is increased. Larger amounts of Cr at the surface increase the acidity of the catalyst which may promote the formation of hydrocarbons relative to alcohols. The addition of larger amounts of alkali to the catalyst may inhibit the formation of hydrocarbons simply by blocking the surface Cr species. Surface characterization studies have demonstrated that the alkali is typically bound to the Cr species in the near-surface region which indicates that this may indeed be the cause for the suppressed hydrocarbon formation. This is not the only role of the alkali promotor, however. A previous study has demonstrated that a nonpromoted ZnO powder is only active toward HAS when promoted with K (7). Therefore, the K may suppress hydrocarbon formation through site blocking, but it also contributes in a different manner toward the production of alcohols, possibly through an electronic modification of the surface.

The product stream composition for the Cs-promoted catalysts at the four different operating conditions is shown in Table 3. The lowest hydrocarbon by-product rates occur at 1000 psig and 400°C. This setting again results in the lowest isobutanol production rates. The highest selectivities consistently occur at 400°C since the greatest amounts of methanol and lowest hydrocarbon by-product rates are produced at this setting. The highest single-pass conversions are

TABLE 3

Product Stream Composition Using a 5.9 wt% Pd/Zn/Cr Spinel Containing Excess ZnO and Promoted with

	1 wt% Cs				3 wt% Cs				5 wt% Cs			
P(psig)	1000	1500	1500	1000	1000	1500	1500	1000	1000	1500	1500	1000
T(°C)	400	400	440	440	400	400	440	440	400	400	440	440
Selectivity to total alcohols (%)	52	62	43	48	85	84	67	77	91	91	81	88
Total alcohol rate (g/kg-h)	120	230	184	132	193	282	238	228	188	276	233	212
Methanol rate (g/kg-h)	75	158	64	51	71	150	48	32	82	156	45	23
Ethanol rate (g/kg-h)	0	0	9	7	1	3	0	0	0	1	0	0
Isopropanol rate (g/kg-h)	0	0	4	0	1	2	7	4	2	3	10	7
n-Propanol rate (g/kg-h)	0	4	16	12	15	22	22	23	19	26	29	28
Isobutanol rate (g/kg-h)	44	68	91	62	105	105	161	170	84	90	150	154
MeOH/i-ButOH mole ratio	3.9	5.4	1.6	1.9	1.6	3.3	0.69	0.44	2.3	4.0	0.69	0.35
Hydrocarbon rate (g/kg-h)	63	77	154	89	22	31	84	49	11	31	39	22
Conversion (%)	11	13	17	10	17	18	20	19	19	18	19	18

found at the higher settings of 1500 psig and 440°C, as are the highest hydrocarbon by-product rates, which contribute to the increased conversion. Previous reaction studies demonstrate that the higher temperature and pressure settings result in the largest isobutanol production rates (5–8). The addition of the Pd and the larger Cs amounts of 3 and 5 wt% to the excess ZnO-containing catalysts produce the highest isobutanol production rates at the lower pressure of 1000 psig. This reduction in operating pressure is economically beneficial with regard to processing. Furthermore, methanol-to-isobutanol mole ratios of less than one are obtained at the lower pressure for the 3 and 5 wt% Cs-promoted catalysts. Significant amounts of *n*-propanol are also produced over these catalysts, and the highest *n*-propanol production rates are typically achieved at 440°C and 1500 psig.

The total alcohol production rate as a function of the Cs loading on the Pd-promoted Zn/Cr catalysts at 440°C and 1500 psig is shown in Fig. 1a. The addition of 1 wt% Cs promotor yields an increase in the total alcohol rate as does the addition of 3 wt% Cs yielding 238 g/kg-h of alcohols. Further Cs promotion of 5 wt% results in a decrease in the total alcohol production rate to 233 g/kg-h. The separate methanol and isobutanol production rates as a function of the Cs loading are shown in Fig. 1b. Similar to the total alcohol production rate data, the isobutanol production rate increases with the addition of 1 and 3 wt% Cs to 91 and 161 g/kg-h, respectively, but decreases with the addition of 5 wt%. The amount of methanol produced decreases with increasing amounts of Cs. The combination of the decreasing methanol and isobutanol production rates at the 5 wt% loading results in the decrease of total alcohol production observed in Fig. 1a. Since the higher isobutanol production rates are obtained at 1000 psig for the 3 and 5 wt% Cs-promoted samples, data obtained as a function of Cs loading at this pressure and 440°C are shown in Fig. 1 as well. The addition of 1 wt% Cs results in a large decrease in the total alcohol production rate. Otherwise, the trends match those observed at the higher pressure of 1500 psig. Larger amounts of isobutanol are formed with the 3 and 5 wt% promoted Cs catalysts at 1000 psig, compared to the amounts formed at 1500 psig, but the total alcohol production rates are consistently lower due to the smaller methanol production rates. The production of 170 g/kg-h of isobutanol is greater than the values obtained using these operating conditions with other types of catalysts (5–9), even at the higher pressure setting. Most importantly, it is greater than other values presented in the literature (2,4,12–22). The effects of Cs loading on the selectivity to total alcohols at 440°C and both 1000 and 1500 psig are shown in Fig. 2a. Similar to K promotion, increasing the Cs promotor concentration results in increased selectivity and decreased hydrocarbon byproduct rates. Using the 5 wt% Cs-promoted catalyst at 440°C and 1000 psig, a selectivity of 88% and a hydrocarbon byproduct rate of 22 g/kg-h are obtained. Also, the hydrocarbon by-product rates are consistently smaller at the lower pressure so the selectivities are consistently higher. Furthermore Figs. 1 and 2 demonstrate that the use of Cs as the promotor results in better catalytic performance, compared to K, which is consistent with the results of previous studies (6,8,9,12).

A summary of the results obtained from various catalysts tested in this series of experiments is shown in Table 4. Results from catalysts which yield the highest isobutanol production rates from each study are shown. These data verify that the addition of Pd and excess ZnO result in improved catalyst performance. Although 171 g/kg-h of isobutanol are produced using a 3 wt% Cs-promoted Zn/Cr catalyst containing excess ZnO and no Pd, this production rate occurs at the higher pressure of 1500 psig, and at 1000 psig only 120 g/kg-h of isobutanol are produced (8). This series of studies, in which both surface characterization techniques, as well as reaction studies, were employed, has resulted in a 47% increase in the isobutanol production, compared to the initial studies which tested the performance of K- and Cs-promoted, commercially available Zn/Cr spinel catalysts (5,6).

Characterization Studies

As-prepared and pretreated catalysts. The 5 wt% K-promoted/5.9 wt% Pd-promoted Zn/Cr catalyst and the 3 wt% Cs-promoted/5.9 wt% Pd-promoted Zn/Cr catalyst were selected for the surface characterization studies because they yield high isobutanol production rates, large selectivities to total alcohols, low methanol-to-isobutanol mole ratios, and low hydrocarbon by-product rates. An XPS survey spectrum taken from the fresh K-promoted catalyst is shown in Fig. 3a. Features due to Zn and O are readily

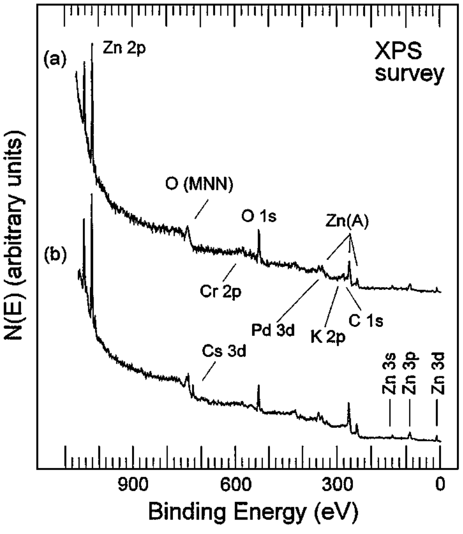

FIG. 3. XPS survey spectra obtained from the (a) 5 wt% K-promoted and (b) 3 wt% Cs-promoted/5.9 wt% Pd-promoted Zn/Cr catalysts containing excess ZnO before pretreatment.

TABLE 4

Summary of Product Stream Compositions Obtained Using the Catalysts Tested as Part of This Series of Experiments at 440°C and 1500 psig (Except for * Which Was Operated at 1000 psig)

Catalyst (Ref. number in parenthesis)	Methanol rate (g/kg-h)	Isobutanol rate (g/kg-h)	Total alcohol rate (g/kg-h)	Selectivity to total alcohols (%)	Hydrocarbon rate (g/kg-h)	Methanol-to-isobutanol mole ratio[a]
1 wt% K/Zn/Cr Engelhard spinel (5)	49	103	167	53	101	1.1
3 wt% Cs/Zn/Cr Engelhard spinel (6)	48	116	214	81	35	0.96
1 wt% K/ZnO (7)	42	38	85	70	23	2.6
3 wt% K/Zn/Cr (1 : 1 Zn : Cr) (8)	39	90	131	64	47	1.0
5 wt% Cs/Zn/Cr (1 : 1 Zn : Cr) (8)	74	133	242	59	112	1.3
5 wt% K/Zn/Cr (excess ZnO) (8)	47	117	178	71	48	0.93
3 wt% Cs/Zn/Cr (excess ZnO) (8)	58	171	248	77	52	0.78
5 wt% Cs/5.9 wt% Pd/Zn/Cr (1 : 1 Zn : Cr) (11)	36	142	227	68	77	0.59
3 wt% K/5.9 wt% Pd/Zn/Cr (excess ZnO)	54	136	221	57	111	0.92
5 wt% Cs/5.9 wt% Pd/Zn/Cr (excess ZnO)*	32	170	228	77	49	0.44
1 wt% Cs/Zn/Cr/Mn (excess ZnO) (23)	50	96	153	67	49	1.2

[a] The methanol-to-isobutanol mole ratios in previous parts of this study have been incorrectly reported due to a software error. The values which are listed in Refs. 5–9 should be multiplied by 0.58 to obtain the correct ratio.

apparent, as are small C and Cr features. No distinct K 2p peaks or Pd 3d peaks, which would be located at binding energy (BE) values of approximately 292–297 eV and 335–340 eV, respectively, are discernible in this spectrum. The near-surface region of this catalyst contains primarily Zn and O, and although prepared with 5.9 wt% Pd and a 1 : 3 weight ratio of Cr to Zn, very little Cr and Pd are evident. The survey spectrum obtained from the Cs-promoted catalyst is shown in Fig. 3b. Again the primary features are due to Zn and O, although a Cs peak is observable while no C feature is apparent. The survey spectra obtained from the pretreated and aged catalysts are very similar so they are not presented. The only differences are the relative intensities of the peaks. Pretreating the catalysts in 1×10^{-7} Torr of H_2 at 300°C for 4 h results in significant increases in the K or Cs signals, relative to the Zn and O features. The amount of Cr in the near-surface region of the Cs-promoted catalyst appears to be unaffected by the pretreatment while the K-promoted catalyst contains more Cr in the near-surface region after the pretreatment. The spectra taken from the catalysts after aging for 5 days indicate that the near-surface Cr concentration also increases during the reaction process. Furthermore, after aging the amount of Cs in the near-surface region increases relative to Zn, and the amount of K in the near-surface region of the K-promoted sample decreases relative to Zn.

A high-resolution Zn 2p XPS spectrum taken from the K-promoted catalyst is shown in Fig. 4a. The predominant feature has a binding energy (BE) value of 1021.7 eV that corresponds to that of ZnO (24). The spectrum denoted by the dotted line, also shown in this figure, was obtained from a K-promoted ZnO powder sample (7) and is used as a basis of comparison in this figure. The broadening of the signal at the higher-BE region of the spectrum obtained from the K-promoted Pd/Zn/Cr catalyst is attributed to the presence of Zn hydroxide states, and the broadening on the lower-BE side is due to the presence of the $ZnCr_2O_4$ (25) spinel support material which resides near the surface of these samples. The spectrum taken from the catalyst after pretreatment in 1×10^{-7} Torr of H_2 for 4 h at 300°C is shown in Fig. 4b. Again, the primary state of the Zn is ZnO as it is after sputtering with 1-keV He ions for 5 min and for an additional 15 min with a 1-keV mixture of He^+ and Ar^+ (Fig. 4c). Previous surface characterization studies of the Zn/Cr-based catalyst systems exhibit similar trends (5–7,9,26) in that ZnO is the predominant Zn species in the near-surface region of these HAS catalysts. The intensity of the signal originating from Zn hydroxide is decreased after pretreating the catalyst in the reductive environment,

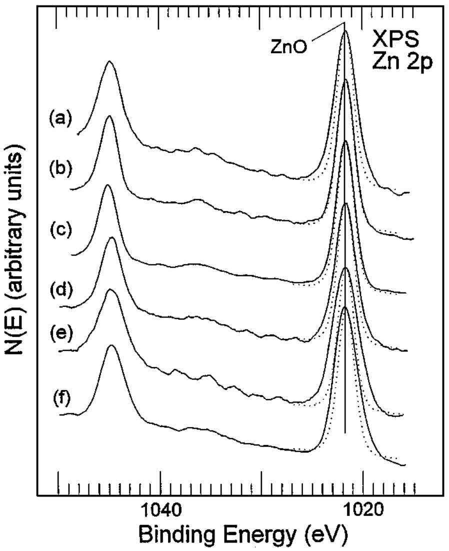

FIG. 4. High-resolution XPS Zn 2p spectra obtained from the 5 wt% K-promoted Pd/Zn/Cr catalyst after (a) insertion into the UHV analysis chamber, (b) pretreatment in 1×10^{-7} Torr of H_2 at 300°C for 4 h, and (c) sputtering with 1-keV He^+ for 5 min and a 1 : 1 mixture of 1 keV Ar^+ and He^+ for 15 min and spectra obtained from the 3 wt% Cs-promoted Pd/Zn/Cr catalyst after (d) insertion into the UHV analysis chamber, (e) pretreatment in 1×10^{-7} Torr of H_2 at 300°C for 4 h, and (f) sputtering with 1-keV He^+ for 15 min and a 1 : 1 mixture of 1 keV Ar^+ and He^+ for 15 min.

most probably through the formation and then desorption of water. The contribution from Zn/Cr spinel is also decreased, indicating that pretreatment produces a film of ZnO which covers the spinel. The spectrum shown in Fig. 4c was obtained after sputtering the surface for 5 min with 1-keV He^+ and for 15 min with a 1-keV mixture of 1 : 1 He^+ and Ar^+. The hydroxide contribution is slightly increased due to exposure of subsurface hydroxyl groups, and some of the ZnO is removed so there is a slightly increased contribution from $ZnCr_2O_4$. The Zn 2p XPS spectrum obtained from the fresh, Cs-promoted catalyst is shown in Fig. 4d. Similar to the K-promoted catalyst, the primary state of Zn in the near-surface region of this catalyst is again ZnO, while contributions from small amounts of Zn hydroxide and $ZnCr_2O_4$ species are also apparent. The fresh Cs-promoted catalyst does contain a slightly smaller amount of Zn hydroxide, compared to the K-promoted catalyst, although the pretreatment produces increases in both the amounts of hydroxide and $ZnCr_2O_4$ (Fig. 4e), which is opposite to that of the behavior of the K-promoted catalyst. The sputtering process reduces the amount of Zn hydroxide in the near-surface region of the Cs-promoted catalyst, as seen by comparing the Zn 2p spectra shown in Figs. 4e and 4f which were obtained from the pretreated sample before and after sputtering for 20 min with 1-keV He^+ and for an additional 15 min with a 1-keV mixture of 1 : 1 He^+ and Ar^+. These data indicate that Zn hydroxide resides primarily near the surface and is removed quickly by the sputtering process. The spinel contribution is also decreased by the sputtering process. These data suggest that the ZnO layer formed after reductive pretreatment in this case is not as thick. The reduction in the spinel contribution may be due to conversion of $ZnCr_2O_4$ to ZnO by sputtering.

An O 1s spectrum obtained from the K-promoted catalyst is shown in Fig. 5a. The oxygen in the near-surface region of this sample is bound as hydroxyl groups, adsorbed water, $ZnCr_2O_4$, and ZnO. The peak is quite broad, and it is not possible to determine the relative amounts of the various species. The predominant species are ZnO, OH^-, and surface water. Their contributions seem to give the broad feature with an apparent peak maximum due to spinel even though spinel is present in smaller quantities. K_2CrO_4 and $K_2Cr_2O_7$ have O 1s BE values of 530.3 and 530.5 eV, respectively (27,28), but these are not observed because they are present in small quantities and lie near the more intense ZnO feature. After pretreating the catalyst the amount of near-surface water and hydroxyl species diminish relative to the ZnO as observed by comparing Fig. 5b with Fig. 5a. Clearly, most of the oxygen is now bound as ZnO. These data correlate well with the Zn 2p data discussed above indicating that the hydroxyl groups observed in Fig. 5a are mostly associated with the Zn. The pretreatment reduces the amount of Zn hydroxide species resulting in the smaller hydroxyl contributions in the O 1s feature and at the higher

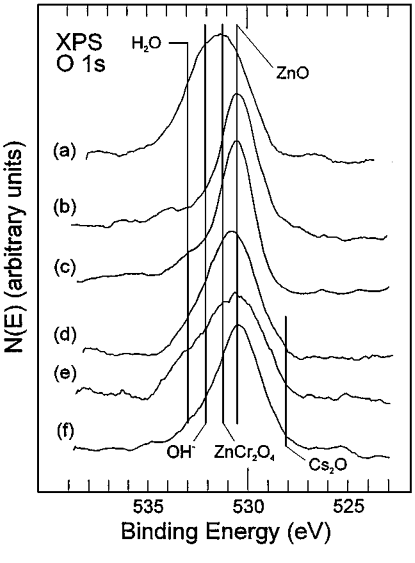

FIG. 5. High-resolution XPS O 1s spectra obtained from the 5 wt% K-promoted Pd/Zn/Cr catalyst after (a) insertion into the UHV analysis chamber, (b) pretreatment in 1×10^{-7} Torr of H_2 at 300°C for 4 h, and (c) sputtering with 1-keV He^+ for 5 min and a 1 : 1 mixture of 1-keV Ar^+ and He^+ for 15 min and spectra obtained from the 3 wt% Cs-promoted Pd/Zn/Cr catalyst after (d) insertion into the UHV analysis chamber, (e) pretreatment in 1×10^{-7} Torr of H_2 at 300°C for 4 h, and (f) sputtering with 1-keV He^+ for 15 min and a 1 : 1 mixture of 1-keV Ar^+ and He^+ for 15 min.

BE side of the corresponding Zn 2p feature. No O contribution due to spinel is apparent, which is consistent with the Zn 2p spectra. According to the spectrum shown in Fig. 5c, the sputtering process causes the near-surface hydroxyl and adsorbed water concentrations to increase relative to the ZnO, which is consistent with the discussion above regarding the Zn 2p peaks.

The O 1s spectrum obtained from the Cs-promoted catalyst is shown in Fig. 5d. Similar to that in Fig. 5a, H_2O, OH^-, $ZnCr_2O_4$, and ZnO species are all present, but less OH^-, H_2O, and $ZrCr_2O_4$ are present in this case, which is consistent with the interpretation of the Zn 2p spectra. The spectrum shown in Fig. 5e was obtained from the pretreated, Cs-promoted catalyst. According to the survey spectra (not shown) this feature is similar in size to that in Fig. 5d, but it is broadened on the high-BE side due to the creation of surface hydroxyl groups and water during the reductive pretreatment in hydrogen. The corresponding Zn 2p spectrum (Fig. 4e) contains an enhanced contribution from the presence of Zn hydroxide as well, and a shoulder due to spinel is apparent, which also is in agreement with the corresponding Zn 2p data in Fig. 4. After sputtering the pretreated, Cs-promoted catalyst for 20 min with 1-keV He^+ and then 15 min with a 1 : 1 He^+ and Ar^+ mixture, the O 1s spectrum shown in Fig. 5f was taken. The differences between this spectrum and that in Fig. 5e indicate that the sputtering process removes surface water and hydroxyl groups which reside near the surface above a ZnO-enriched layer. This result also is consistent with the analysis of the Zn 2p spectra discussed above. One difference between the K- and Cs-promoted catalysts is the amount of hydroxyl species which are present. The pretreated Cs-promoted catalyst surface contains more OH^- species than the surface of the pretreated K-promoted catalyst which may be responsible for the greater catalytic activity associated with Cs promotion. Surface characterization data obtained from similar, Cs-containing catalysts have contained evidence of Cs_2O stabilized in the near-surface region of these samples (6,11). This feature appears to be present in this study, but it is very small.

A high-resolution Cr 2p XPS spectrum obtained from the K-promoted, catalyst is shown in Fig. 6a. The signal-to-noise ratios of the spectra presented in Fig. 6 are quite low due to the small amounts of Cr present in these near-surface regions. These catalysts were made with an excess amount of Zn (3 : 1 Zn : Cr) and as shown in a previous study (5) the near-surface region of even the 1 : 1 Zn : Cr spinel material contains significantly larger amounts of Zn. Although the signal-to-noise are low, some features may be meaningful. Several Cr species are probably present including chromate, dichromate, spinel, and oxides. Pretreating the catalyst significantly increases the amounts of $K_2Cr_2O_7$ and K_2CrO_4 present as shown in Fig. 6b, and these species are still present after sputtering. A Cr 2p XPS spectrum obtained from the Cs-promoted catalyst is shown in Fig. 6d. It has a similar shape to that obtained from the fresh K-promoted catalyst. Pretreatment causes a reduction in Cr signal strength (Fig. 6e), and sputtering results in an increase with chromates/dichromates and spinel predominating. The near-surface region of the Cs-promoted catalyst contains less Cr than the K-promoted catalyst, which explains the smaller amounts of hydrocarbon byproducts obtained using the Cs-promoted catalyst as shown in Fig. 2.

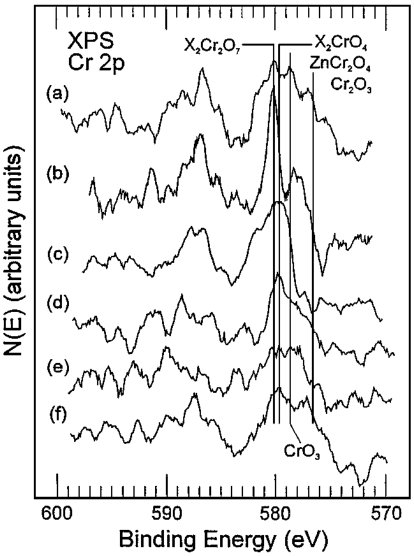

FIG. 6. High-resolution XPS Cr 2p spectra obtained from the 5 wt% K-promoted Pd/Zn/Cr catalyst after (a) insertion into the UHV analysis chamber, (b) pretreatment in 1×10^{-7} Torr of H_2 at 300°C for 4 h, and (c) sputtering with 1-keV He^+ for 5 min and a 1 : 1 mixture of 1-keV Ar^+ and He^+ for 15 min and spectra obtained from the 3 wt% Cs-promoted Pd/Zn/Cr catalyst after (d) insertion into the UHV analysis chamber, (e) pretreatment in 1×10^{-7} Torr of H_2 at 300°C for 4 h, and (f) sputtering with 1-keV He^+ for 15 min and a 1 : 1 mixture of 1-keV Ar^+ and He^+ for 15 min.

An XPS Pd 3d and Zn(LMM) spectrum obtained from the fresh K-promoted catalyst is shown in Fig. 7a. PdO_2 is the predominant Pd state present in the near-surface region, and very small amounts of PdO and Pd^0 may also be present. The spectrum shown in Fig. 7b was obtained from the K-promoted sample after the reductive pretreatment. The Pd peak is now larger relative to the Zn (LMM) peaks, indicating that the pretreatment causes subsurface Pd to migrate toward the surface or that near-surface O and/or C species are removed, exposing the subsurface Pd. Apparently, all of the Pd is present as PdO_2. Sputtering the pretreated sample results in loss of near-surface Pd relative to the Zn and reduction of some PdO_2 to PdO, as shown in Fig. 7c. These results imply that the near-surface region of the pretreated catalyst contains a layer enriched in Pd which is quickly removed by sputtering. The Pd 3d spectrum obtained from the fresh Cs-promoted catalyst is shown in Fig. 7d. A much smaller amount of Pd is present

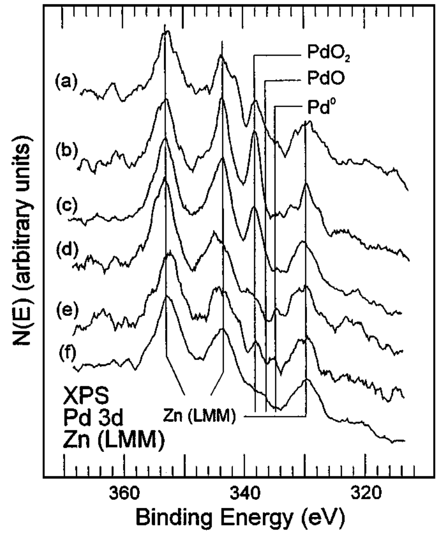

FIG. 7. High-resolution XPS Pd 3d spectra obtained from the 5 wt% K-promoted Pd/Zn/Cr catalyst after (a) insertion into the UHV analysis chamber, (b) pretreatment in 1×10^{-7} Torr of H_2 at 300°C for 4 h, and (c) sputtering with 1-keV He^+ for 5 min and a 1 : 1 mixture of 1-keV Ar^+ and He^+ for 15 min and spectra obtained from the 3 wt% Cs-promoted Pd/Zn/Cr catalyst after (d) insertion into the UHV analysis chamber, (e) pretreatment in 1×10^{-7} Torr of H_2 at 300°C for 4 h, and (f) sputtering with 1-keV He^+ for 15 min and a 1 : 1 mixture of 1-keV Ar^+ and He^+ for 15 min.

in the near-surface region, compared to the K-containing catalyst. In addition to PdO_2, there is a small but distinct feature due to the presence of Pd metal at 334.8 eV. As shown in Fig. 7e, the reductive pretreatment results in a small enrichment in the Pd content of the near-surface region. The PdO_2 feature is more well defined, but the intensity of the Pd metal signal is not altered. The sputtering process almost eliminates the Pd from the near-surface region of the Cs-promoted catalyst (Fig. 7f). The results from both the K- and Cs-containing catalysts demonstrate that an enriched Pd layer exists near the surfaces of these catalysts after the pretreatment. However, differences do exist between the amounts and chemical states of Pd present on the K- and Cs-promoted samples. On both catalysts PdO_2 is predominant, but more Pd metal is present on the Cs-promoted catalyst. Using the Zn (LMM) signal as a measure, considerably more Pd is present on the surface of the K-promoted catalyst. Pd is an important component in many catalysts used for hydrogenation and both CO and methane oxidation (C-H bond breakage). Although the role of Pd is not understood yet with regard to HAS, all of these functions could be important.

A high-resolution XPS C 1s and K 2p spectrum taken from the fresh K-promoted catalyst is shown in Fig. 8a. This spectrum conveys little information since the signals are so small due both to low sensitivity factors and low concentrations. The carbon originates from contaminants which accumulate either during preparation or air exposure. Alcohol and hydrocarbon contaminants are typically observed after such air exposures. These contaminants are removed from the K-promoted catalyst by the reductive treatment (Fig. 8b) and sputtering does not alter the amount of the carbon present as expected (Fig. 8c). A C 1s spectrum obtained from the Cs-promoted catalyst is shown in Fig. 8d. Even less carbon is present in this case, and it also is present in the form of alcohol and hydrocarbon contaminants. The spectrum shown in Fig. 8e was obtained after the reductive pretreatment. Hydrocarbons are no longer present, but some alcohols may still be present. Sputtering the pretreated catalyst eliminates the carbon species (Fig. 8f). These data indicate that the small amounts of carbon contaminants associated with K-promoted catalyst reside at the surface and are not distributed through the underlying layers.

According to the XPS data shown in Fig. 8a obtained from the fresh K-promoted catalyst, the small amount of K present is apparently bound to the Cr as a chromate or dichromate species (27,28), which is consistent with the corresponding Cr 2p spectrum discussed above. The reductive pretreatment significantly increases the concentration of the potassium dichromate species (Fig. 8b). The K 2p XPS data shown in Fig. 8c was taken after sputtering the catalyst for 5 min with 1-keV He^+ and an additional 15 min with a 1-keV mixture of 1 : 1 He^+ and Ar^+. The sputtering process removes much of the K in the near-surface region, which indicates that the K resides primarily at the surface

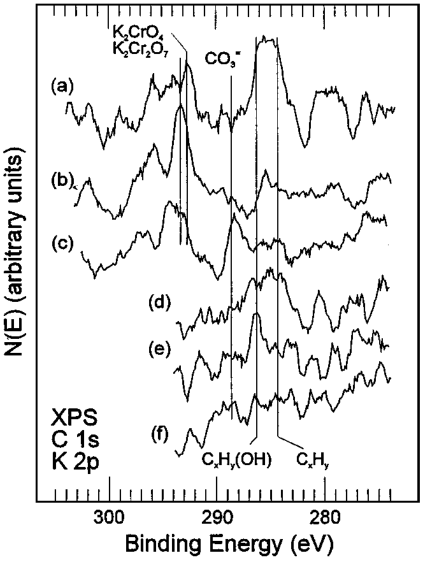

FIG. 8. High-resolution XPS C 1s (and K 2p) spectra obtained from the 5 wt% K-promoted Pd/Zn/Cr catalyst after (a) insertion into the UHV analysis chamber, (b) pretreatment in 1×10^{-7} Torr of H_2 at 300°C for 4 h, and (c) sputtering with 1-keV He^+ for 5 min and a 1 : 1 mixture of 1-keV Ar^+ and He^+ for 15 min and spectra obtained from the 3 wt% Cs-promoted Pd/Zn/Cr catalyst after (d) insertion into the UHV analysis chamber, (e) pretreatment in 1×10^{-7} Torr of H_2 at 300°C for 4 h, and (f) sputtering with 1-keV He^+ for 15 min and a 1 : 1 mixture of 1-keV Ar^+ and He^+ for 15 min.

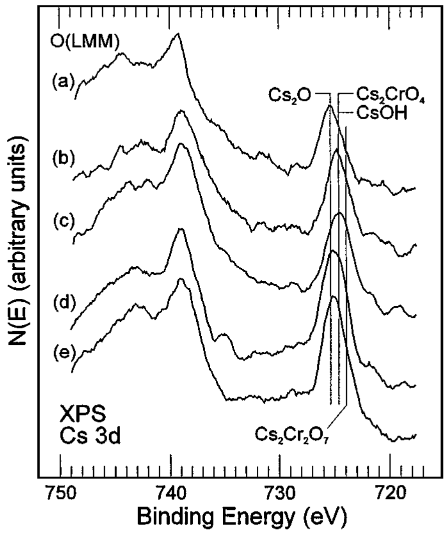

FIG. 9. High-resolution XPS Cs 3d spectra obtained from the 3 wt% Cs-promoted Pd/Zn/Cr catalyst after (a) insertion into the UHV analysis chamber, (b) pretreatment in 1×10^{-7} Torr of H_2 at 300°C for 4 h, and (c) sputtering with 1-keV He^+ for 5 min and a 1:1 mixture of 1-keV Ar^+ and He^+ for 15 min, (d) aging in the reactor for 5 days, and sputtering the Cs-promoted, aged catalyst for 30 min with 1-keV He^+.

of this sample. This result coincides with the corresponding Cr 2p data, where a decrease in the concentration of the Cr states associated with the K is observed. However, the Cr concentration is increased, as evidenced by comparing the Cr features in the survey spectra obtained before and after sputtering. This is reasonable since Cr-containing spinel lies beneath the alkali, ZnO, and Pd. Cr 2p peaks due to spinel are not apparent in Fig. 6c, indicating that ion sputtering decomposes spinel. A high-resolution Cs 3d XPS spectrum obtained from the fresh Cs-promoted catalyst is shown in Fig. 9a. O (LMM) peaks are also present at binding energies above 735 eV. The Cs in the near-surface region of the fresh catalyst consists of a mixture of chemical states including Cs_2O, CsOH, or Cs_2CrO_4 and $Cs_2Cr_2O_7$. Cs_2O is not considered to be a stable species in an UHV environment. This fact suggests that another chemical state of Cs may have a BE close to that of Cs_2O or that Cs_2O is stabilized at this surface. The spectrum shown in Fig. 9b was obtained after the reductive pretreatment. The increased size of the Cs peaks relative to the O (LMM) feature and the noise level indicates that this pretreatment causes an increase in the near-surface region Cs concentration. Furthermore, the relative amounts of the various Cs chemical states are changed. The O 1s data discussed above exhibit an increase in the concentration of OH^- groups, and the Cr 2p data exhibit an increase in Cs_2CrO_4. Therefore, the increased signal intensity at a BE value of 724.5 eV is most likely due to increased amounts of both Cs_2CrO_4 and CsOH. As shown in Fig. 9c, sputtering the pretreated catalyst surface results in little change in the chemical species distribution, but the Cs concentration is decreased. This indicates that the distribution of Cs states throughout the near-surface region is fairly homogeneous. A decrease in the OH^- contribution to the corresponding O 1s spectrum (Fig. 5c) is observed, and the amount of Zn hydroxide also is decreased. The remaining OH^- signal could be associated with the CsOH. The fact that no increase is observed in the Cs_2CrO_4 Cr 2p signal which would offset an intensity decrease in the Cs 3d signal supports this assertion.

Ion scattering spectroscopy (ISS) is a very important surface characterization technique which provides compositional information concerning the outermost atomic layer of a sample (29). This data is most useful for studying catalytic materials since this is the region where catalytic reactions occur. An ISS spectrum obtained from the fresh K-promoted catalyst is shown in Fig. 10a. The largest feature in this spectrum is centered at an E/E_0 value of approximately 0.58. It results from sample charging due to the insulating nature of this surface. Elements with features near this peak cannot be observed due to overlapping with this large charging feature. A large oxygen feature is evident, as are small peaks due to Pd and Zn. However, K or Cr features are not observable. Sample charging is often accompanied by a large O feature. The ISS spectrum shown in Figure 10b was obtained after pretreating the catalyst in 10^{-7} Torr of H_2 at 300°C. The charging feature is shifted to a lower E/E_0, and it is still quite intense. No distinct O feature is present indicating that oxygen is removed from the outermost surface layer during the pretreatment, although

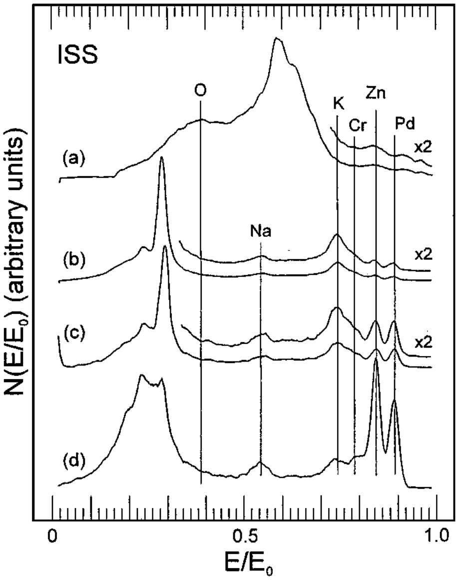

FIG. 10. ISS spectra obtained from the 5 wt% K-promoted Pd/Zn/Cr catalyst after (a) insertion into the UHV analysis chamber, (b) pretreatment in 1×10^{-7} Torr of H_2 at 300°C for 4 h, (c) sputtering the pretreated catalyst for 5 min with 1-keV He^+, and (d) sputtering for an additional 15 min with a mixture of 1-keV 1:1 He^+ and Ar^+.

significant quantities of oxygen are present beneath the surface according to XPS. The Zn and Pd peaks are also still present, and now Cr and K features are observable also. Furthermore, a small Na peak is present. This contaminant most likely originates from the sample preparation process. These results, in conjunction with the XPS results discussed above, indicate that the as-prepared surface contains little or no K promotor and that the pretreatment causes the subsurface K, bound through the Cr, to migrate toward the sample surface, or more likely, that these species lie just beneath the O which is removed during pretreatment. ISS spectra were also taken after various sputter times, and two representative spectra are shown in Figs. 10c and d. These were obtained after sputtering for 5 min with 1-keV He^+ and then after an additional 15 min of sputtering with a 1-keV mixture of 1 : 1 He^+ and Ar^+, respectively. After 5 min of sputtering, the Zn and Pd peaks are increased relative to the K feature, and both peaks are more intense and well defined. A very small oxygen feature is also apparent. This indicates that the oxygen does reside beneath the outermost atomic layer after the pretreatment. However, O is most likely sputtered away preferentially. Further sputtering results in large increases in the Zn and Pd features relative to the K and Cr peaks (Fig. 10d), indicating that an enriched K layer exists near the surface of the pretreated catalyst. Continued sputtering results in a decrease in the Pd peak intensity relative to the Zn. Apparently, Na is distributed throughout the near-surface region. This qualitative depth profile using ISS and XPS indicates that the pretreated catalyst consists of a K-enriched layer at the surface, bound to Cr. As the K is removed by the sputtering process, an enriched Pd layer is exposed which resides above the Zn/Cr support material. A ZnO-enriched layer lies beneath the Pd.

An ISS spectrum obtained from the fresh Cs-promoted catalyst is shown in Fig. 11a. A large, broad feature is present at an E/E_0 value of approximately 0.28. This feature is due to large quantities of C and O in the outermost atomic layer. Distinct features are evident due to the presence of Na and Zn at the outermost surface layer. The high E/E_0 feature consists of both Pd and Cs with the Cs peak lying at a higher E/E_0 since it has a higher mass than Pd. The reaction data presented above indicate that the bare support catalyzes the synthesis of higher alcohols even when no Cs promotor is added. The spectrum shown here contains a Na contaminant feature, and the Na is an alkali promotor for HAS (12,24), which explains the activity associated with the nonpromoted catalyst materials. The ISS spectrum shown in Fig. 11b was obtained after the reductive pretreatment. The Pd/Cs feature is now larger in size relative to the Zn feature, which is barely apparent. The increase in the Pd/Cs feature is most likely due to an increase in the Cs, based on the behavior of the K-promoted catalyst. As discussed above, a slight increase in the near-surface Pd concentration is observed in the corresponding Pd XPS spectra. These facts suggest that Pd lies just beneath the alkali. The Na peak is more prominent also, and the O feature is reduced in intensity. The feature due to sample charging is apparent at a lower E/E_0 value. A small Cr feature is also present. The ISS spectrum obtained from the pretreated K-promoted catalyst contains signal contributions from Zn and Cr as well, indicating that the outermost atomic layer of that catalyst is not completely covered by the K and Pd promotors. In ISS the cross section increases with mass so the cross section for Cs is greater than that of K. Since accurate cross sections are not available, it is not possible to determine the relative alkali coverages on the pretreated K- and Cs-promoted catalyst. Sputtering the pretreated sample for 5 min with 1-keV He^+ results in increases in the Zn and the Cr signals relative to the Cs/Pd feature (Fig. 11c), as expected. The Na feature apparently remains unchanged. The ISS spectrum shown in Fig. 11d was taken from the pretreated catalyst after sputtering for 5 min with 1-keV He^+ and 15 min with a 1-keV mixture of 1 : 1 He^+ and Ar^+. The intensity of the Cs/Pd peak is now decreased relative to the Zn and Cr features. Furthermore, the Na peak is increased in size. These data indicate that a layered structure exists in the near-surface region of the pretreated Cs-promoted catalyst. The outermost surface layer is enriched in Cs and Pd relative to the Zn and Cr. The sputtering process removes some of this layer, thereby exposing more of the Zn and Cr associated with the support material. Further sputtering reveals a layer which contains more Na than that of the near-surface region.

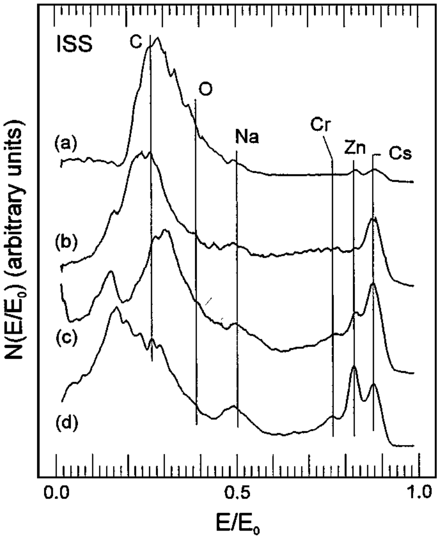

FIG. 11. ISS spectra obtained from the 3 wt% Cs-promoted Pd/Zn/Cr catalyst after (a) insertion into the UHV analysis chamber, (b) pretreatment in 1×10^{-7} Torr of H_2 at 300°C for 4 h, (c) sputtering the pretreated catalyst for 5 min with 1-keV He^+, and (d) sputtering for an additional 15 min with 1-keV He^+ and then a mixture of 1 : 1 He^+ and Ar^+ for 15 min.

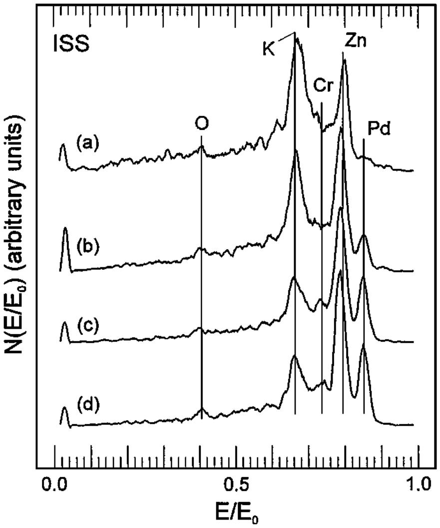

FIG. 12. ISS spectra obtained from the 5 wt% K-promoted Pd/Zn/Cr catalyst after (a) removal from the reactor after 5 days of exposure to reaction conditions, (b) sputtering the aged catalyst for 3.5 min with 1-keV He$^+$, and sputtering the aged catalyst for an additional (c) 11.5 min, and then (d) another 9 min.

Aged catalysts. An ISS spectrum obtained from the K-promoted catalyst after exposure to reaction conditions for 5 days is shown in Fig. 12a. Features are present due to the presence of O, K, Cr, Zn, and Pd at the outermost surface layer. The relative intensities of these peaks differ from those in Fig. 10b obtained from the pretreated sample, indicating that the catalyst surface undergoes changes during the reaction process. The K now covers less of the outermost surface since the Zn feature is increased in size relative to the K, and the Pd peak size is reduced. The sputtering process exposes larger amounts of Pd, Cr, and Zn relative to the K promotor as seen by comparing the ISS spectra obtained after 3.5, 15, and 24 min of sputtering (Figs. 12b, c, and d, respectively). The removal of the K uncovers an underlying layer enriched in Pd and ZnO. The O feature remains relatively unchanged throughout these spectra, suggesting that it is evenly distributed throughout the near-surface region. The K-enriched surface layer is removed more quickly from the aged catalyst, indicating that this layer is now thinner. This conclusion is based on the comparison of the ISS spectra shown in Fig. 10c obtained after 5 min of sputtering and that shown in Fig. 12b obtained after 3.5 min of sputtering under the same conditions. The Zn feature is larger than the K feature in Fig. 12b which is not the case in Fig. 10c. The spectra shown in Fig. 12 do not exhibit charging features indicating that these surfaces are more electrically conductive. Small peaks at low E/E$_0$ are apparent. These are due to secondary ions consisting mostly of H$^+$.

An ISS spectrum obtained from the aged, Cs-promoted catalyst is shown in Fig. 13a. Pd/Cs, Zn, and a small Na peak are present. The Cs-to-Zn peak height ratio is smaller than that of the pretreated sample which again indicates that the amount of alkali is smaller relative to the Zn after exposure to reaction conditions for 5 days. After briefly sputtering the aged catalyst for 66 s, the spectrum shown in Fig. 13b was obtained. No distinct changes are noticeable in the Cs and Zn features, indicating that the outermost atomic layers are uniform with regard to composition. The intensity of the background signal is reduced compared to that of Fig. 13a, indicating that the surface contains less carbon and/or oxygen so that the neutralization efficiency toward He$^+$ which undergoes one or more collisions is greater, resulting in the smaller background. The spectrum shown in Fig. 13c was obtained from the aged catalyst after an additional 29 min of sputtering. The Zn peak is now larger than the Pd/Cs feature, and a Cr feature is evident also. According to these results, the aged sample, much like the pretreated sample, contains an enriched layer of Cs near the surface which covers the Zn and Cr support material. The similar results could explain the lack of catalyst decay over the period tested. A small Na peak is evident in Fig. 13c, indicating that the Na contamination still resides in the aged catalyst but in smaller quantities. A large F peak is also present. This accumulated during the long sputtering period from the background gas because a AgF decomposition experiment was performed in the UHV system just prior to these studies. The presence of the F contaminant does not affect the data interpretation.

XPS data were obtained from the aged K- and Cs-promoted catalysts before and after depth profiling. The Zn 2p spectrum obtained from the aged K-promoted sample is shown in Fig. 14a. ZnO is the primary chemical state of Zn in the near-surface region of this sample. However, a

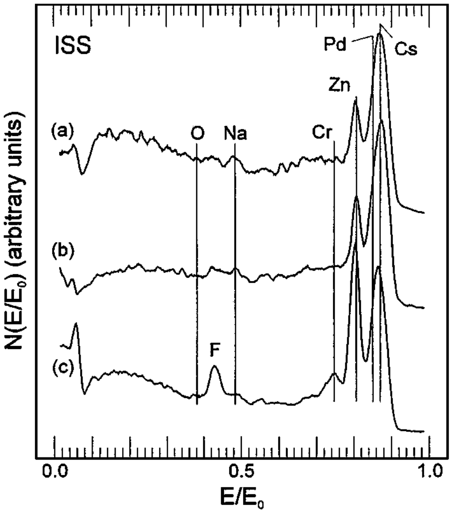

FIG. 13. ISS spectra obtained from the 3 wt% Cs-promoted Pd/Zn/Cr catalyst after (a) removal from the reactor after 5 days of exposure to reaction conditions, (b) sputtering the aged catalyst for 66 s with 1-keV He$^+$, and (c) sputtering the aged catalyst for an additional 29 min.

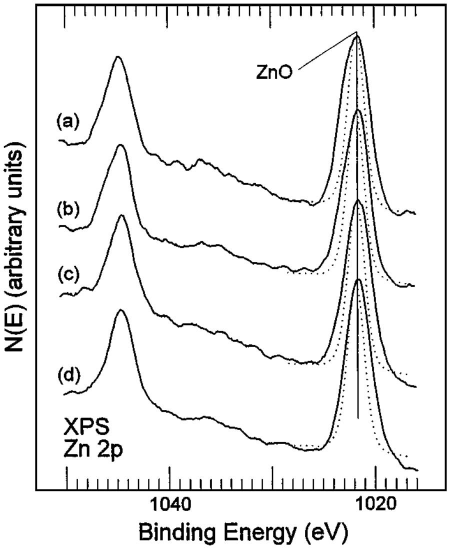

FIG. 14. High-resolution Zn 2p spectra obtained from (a) the 5 wt% K-promoted Pd/Zn/Cr catalyst aging in the reactor for 5 days, (b) after sputtering for K-promoted, aged catalyst for 24 min with 1-keV He^+, (c) the 3 wt% Cs-promoted Pd/Zn/Cr catalyst after aging in the reactor for 5 days, and (d) after sputtering the Cs-promoted, aged catalyst for 30 min with 1-keV He^+.

large amount of Zn hydroxide is present, even more than present on the fresh catalyst. This is consistent with the substantial secondary ion peak in Fig. 12a. The corresponding O 1s spectrum shown in Fig. 15a consists of a broad feature containing large contributions from ZnO, hydroxyl species, water, and probably a smaller spinel contribution. The Zn 2p spectrum is broadened at the lower BE portion which is indicative of the presence of $ZnCr_2O_4$. The surface H_2O may form from the water/gas shift reaction which occurs over these catalysts or through adsorption of atmospheric moisture during the transfer process from the reactor to the UHV analysis system. Sputtering the aged catalyst results in a slight narrowing of the Zn 2p peaks through removal of hydroxyl groups (Fig. 14b). The corresponding O 1s spectrum, shown in Fig. 15b, also contains smaller signal contributions from both the adsorbed H_2O and hydroxyl groups. Compared to the data in Figs. 4b and 5b, taken from the pretreated catalyst before aging, these data indicate that the reaction process depletes the ZnO layer and possibly deposits H_2O and hydroxyl groups on the surface.

A Zn 2p XPS spectrum obtained from the Cs-promoted catalyst after aging in the reactor for 5 days under reaction conditions is shown in Fig. 14c. Again the primary state of the Zn in the near-surface region is ZnO, but less Zn hydroxide is present, compared to the K-promoted catalyst. Sputtering this sample for 30 min with 1-keV He^+ reduces the concentration of the hydroxide state further, as shown in Fig. 14d. The corresponding O 1s spectrum taken from the aged catalyst is shown in Fig. 15c. Most of the oxygen in the near-surface region of the aged Cs-promoted catalyst is bound as ZnO, in contrast to the corresponding spectrum obtained from the K-containing catalyst (Fig. 15a). Significantly smaller concentrations of adsorbed H_2O and hydroxyl groups are present. The lack of these species at or near the surface may correlate with the greater activity associated with the Cs-containing samples. The Cs may inhibit the formation of these species by covering the surface more completely or through an electronic effect. As shown in Fig. 15d, sputtering the catalyst reduces the amount of OH^- groups, in agreement with the corresponding Zn 2p data. This reduction in hydroxyl group concentration causes the small feature due to H_2O to appear more pronounced. In both the Zn 2p spectra obtained from the Cs-containing sample before and after sputtering, a $ZnCr_2O_4$ state is evident. This contribution is increased relative to that of the pretreated catalyst (Fig. 4e), indicating that the reaction process depletes the enriched ZnO layer relative to the $ZnCr_2O_4$ support material. In the O 1s spectrum obtained from the aged, Cs-promoted catalyst (Fig. 15c), there is a greater contribution at the lower BE portion of the spectrum relative to the pretreated sample (Fig. 5e). This is due to the formation of Cs oxide species which are present on the fresh and pretreated surfaces in much smaller quantities. Therefore, the reaction process changes the chemical composition of the oxygen species in the near-surface region, resulting in an increased concentration of Cs_2O.

A Cr 2p XPS spectrum obtained from the aged K-promoted catalyst is shown in Fig. 16a. A mixture of Cr chemical states is present, and the near-surface concentration of the Cr species is greater than that of the fresh pretreated

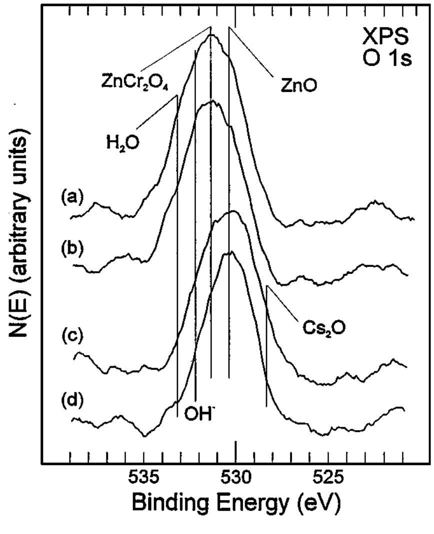

FIG. 15. High-resolution O 1s spectra obtained (a) from the 5 wt% K-promoted Pd/Zn/Cr catalyst after aging under reaction conditions for 5 days, (b) after sputtering the K-promoted, aged catalyst for 24 min with 1-keV He^+, (c) from the 3 wt% Cs-promoted Pd/Zn/Cr catalyst after aging under reaction conditions for 5 days, and (d) after sputtering the Cs-promoted, aged catalyst for 30 min with 1-keV He^+.

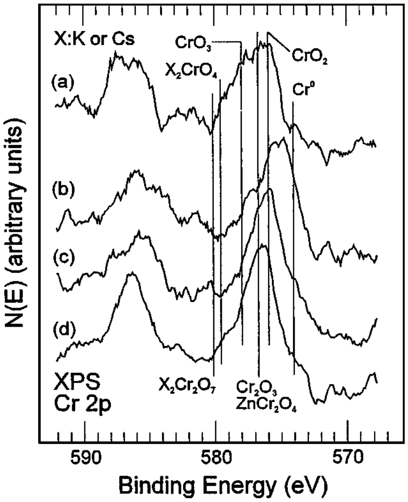

FIG. 16. High-resolution Cr 2p spectra obtained (a) from the 5 wt% K-promoted Pd/Zn/Cr catalyst after aging under reaction conditions for 5 days, (b) after sputtering the aged, K-promoted catalyst for 24 min with 1-keV He$^+$, (c) from the 3 wt% Cs-promoted Pd/Zn/Cr catalyst after aging under reaction conditions for 5 days, and (d) after sputtering the aged, Cs-promoted, catalyst for 30 min with 1-keV He$^+$.

catalyst (Fig. 6b). Most of the Cr is bound as CrO_2, Cr_2O_3, and/or $ZnCr_2O_4$. Smaller amounts of CrO_3 and K_2CrO_4 are also present. The spectrum shown in Fig. 16b was taken from the aged catalyst after sputtering with 1-keV He$^+$ for 24 min. The sputtering process removes much of the near-surface CrO_3, K_2CrO_4, and Cr_2O_3. Since the Zn 2p and O 1s data discussed above do not exhibit a significant decrease in the $ZnCr_2O_4$ concentration, Cr_2O_3 is present in addition to $ZnCr_2O_4$. The Cr 2p XPS spectrum obtained from the aged Cs-promoted catalyst is shown in Fig. 16c. Most of the Cr is bound as CrO_2. Cr_2O_3 and/or $ZnCr_2O_4$, and some metallic Cr is present as well. Sputtering the surface results in a decrease in the CrO_2 concentration and exposure of the underlying $ZnCr_2O_4$ substrate. The sputtering process reveals some Cs_2CrO_4 which resides in the subsurface region after aging. Based on the larger signal-to-noise ratio of this spectrum, more Cr is present in the subsurface region, and all of the Cr signals from the aged catalysts are much stronger than those from the fresh catalysts.

Pd 3d and Zn (LMM) features obtained from the aged K-promoted catalyst are shown in Fig. 17a. Significantly less Pd is present in the near-surface region of this sample, compared to the pretreated sample (Fig. 7b), and it is present as a mixture of PdO and Pd metal rather than PdO_2. However, after sputtering the aged catalyst, a much stronger Pd signal becomes apparent (Fig. 17b). During reaction, the Pd which is initially present in the near-surface region is driven toward the subsurface region, possibly by preferential covering by other species. Furthermore, this Pd is a mixture of Pd^o and PdO with Pd^o predominating. These data in conjunction with the ISS data discussed above suggest that a layer enriched in Pd resides beneath the surface and is exposed with the removal of K. An XPS spectrum obtained from the aged, Cs-promoted catalyst is shown in Fig. 17c. Even less Pd is present in the near-surface region of this sample. The small amount that is present is primarily PdO while some Pd metal is present as well. Sputtering the catalyst does not reveal a larger concentration of Pd beneath the near-surface region as shown in Fig. 17d possibly because the overlying layer formed during reaction is thicker so that the Pd lies further beneath the surface. Somewhat similar results were obtained from a Cs- and Pd-promoted 1 : 1 Zn : Cr spinel catalyst (11) in that the fresh catalyst contains a Pd-enriched layer but the aged sample does not for the sputtering conditions used.

The reaction process involves the formation of various carbon species over these catalysts, including the desired alcohol products and hydrocarbons. An XPS C 1s spectrum obtained from the aged K-promoted sample is shown in Fig. 18a. A large feature which corresponds to alcohol groups is present at a BE of 285.2 eV as expected since most of the reaction products are alcohols. A smaller amount of hydrocarbon species also is present which most likely forms during aging in the reactor but may have accumulated during air exposure upon transfer to the analysis chamber. As shown in Fig. 18b, sputtering the catalyst for 24 min with 1-keV He$^+$ results in a slight decrease in the alcohol concentration, indicating that these species reside at or very near the surface. A C 1s XPS spectrum obtained from the aged Cs-promoted catalyst is shown in Fig. 18c. A substantially smaller amount of carbon is present in the near-surface

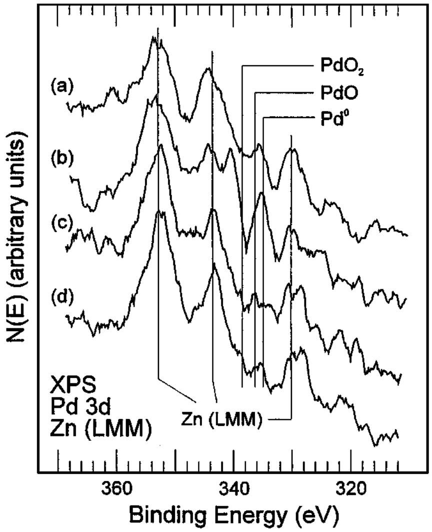

FIG. 17. High-resolution Pd 3d spectra obtained (a) from the 5 wt% K-promoted Pd/Zn/Cr catalyst after aging under reaction conditions for 5 days, (b) after sputtering the K-promoted, aged catalyst for 24 min with 1-keV He$^+$, (c) from the 3 wt% Cs-promoted Pd/Zn/Cr catalyst after aging under reaction conditions for 5 days, and (d) after sputtering the aged, Cs-promoted, catalyst for 30 min with 1-keV He$^+$.

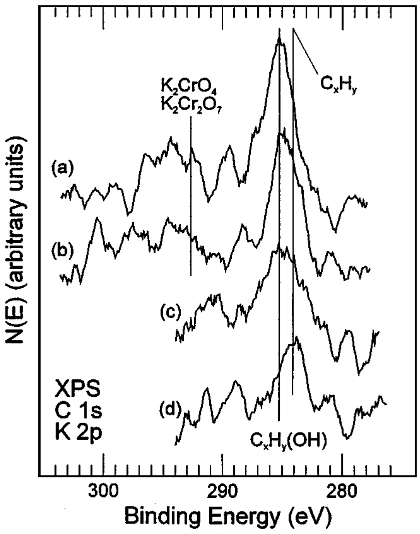

FIG. 18. High-resolution C 1s and K 2p spectra obtained (a) from the 5 wt% K-promoted Pd/Zn/Cr catalyst after aging under reaction conditions for 5 days, (b) after sputtering the K-promoted, aged catalyst for 24 min with 1-keV He^+, (c) from the 3 wt% Cs-promoted Pd/Zn/Cr catalyst after aging under reaction conditions for 5 days, and (d) after sputtering the Cs-promoted, aged catalyst for 30 min with 1-keV He^+.

region of this sample. That which is evident is bound as alcohols and hydrocarbons. Sputtering this catalyst diminishes the amount of alcohol present, indicating that it resides at the surface, but it does not remove the hydrocarbon species as rapidly, suggesting that they lie underneath the alcohols. This assertion is consistent with both sets of spectra shown in Fig. 18. Previous studies have demonstrated that Cs is a superior promotor compared to K (5,6,12). The larger amount of adsorbed carbon species at the surface of the K-containing sample may result in a less active catalyst due to site blocking. Less carbon is present on the Cs-containing catalyst, and therefore more adsorption sites may be available for the reactants, resulting in better catalytic performance.

Although the corresponding ISS spectra (Fig. 12) contains significant contributions due to the presence of K at the surface, very little K-signal contribution is present in the XPS spectra in Fig. 18. XPS and ISS, however, probe quite different regions of the catalyst (29), and therefore differences are expected in nonhomogeneous systems. These XPS data and the depth profile ISS information shown in Fig. 12 indicate that the small amount of K present after aging resides at the catalyst surface. This K-rich layer is thin and quickly removed by the sputtering process, resulting in the loss of the K 2p signal seen in Fig. 18b. The small amount of K species present in the near-surface region is bound primarily as a chromate or dichromate species. The corresponding Cr 2p spectra also contain a very small signal contribution from a K-containing species which correlates with the ISS and XPS data. Furthermore, the amount of K which is present is much smaller than that on the surface of the pretreated, unreacted catalyst (Fig. 8b). Under reaction conditions this catalyst loses the alkali promotor in some manner, but the activity does not decay over the period tested because the remaining K resides at the surface, allowing the reaction to proceed. The Cs 3d XPS spectrum obtained from the aged Cs-containing catalyst is shown in Fig. 9d. Apparently, more Cs is present in the near-surface region since the signal-to-noise ratio is larger, compared to that of Fig. 9b which was obtained from the pretreated sample. Most of the Cs appears to be present as Cs_2O, although a significant amount of Cs_2CrO_4 and/or CsOH is present as well. The corresponding Cr 2p spectrum (Figure 16d) contains a feature which could be attributed to Cs_2CrO_4 which coincides with Cs 3d data. However, it is quite small and only observed after sputtering. A small signal contribution originating from the presence of $Cs_2Cr_2O_7$ is also evident in Fig. 9. As shown in Fig. 9e, sputtering the catalyst results in a slight decrease in the Cs_2O concentration, but it does not seem to affect the amounts of the chromate or hydroxide species. A loss of OH^- groups is observed in the corresponding O 1s spectra, indicating that either these Cs species may be composed primarily of the chromate (or dichromate) species or that most of the OH^- loss occurs through the elimination of Zn hydroxide species. The latter is more likely since very little chromate or dichromate species are present, so this hydroxyl signal must be primarily due to CsOH.

XRD patterns obtained from both the fresh and aged catalysts exhibit features due to Zn/Cr spinel. Since the near-surface region contains mostly ZnO and very little Cr, the structure at the surface is not due to spinel. Based on the results of a study of K-promoted ZnO (no Cr), the function of the Zn/Cr spinel is to provide a high surface-area support for the promoted ZnO.

CONCLUSIONS

K- and Cs-promoted, 5.9 wt% Pd-promoted/Zn/Cr catalysts, containing excess ZnO, were prepared and tested for HAS. Of the catalysts examined under the chosen conditions, the greatest isobutanol production rate is obtained using the 3 wt% Cs-promoted catalyst at 1000 psig and 440°C. In previous related studies higher pressures were required to obtain the highest isobutanol production rates. The addition of the Pd results in a reduction in the optimum operating pressure, which is economically favorable. At these settings 170 g/kg-h of isobutanol is produced. This is significantly greater than other values stated in the literature. A methanol-to-isobutanol mole ratio value of 1.0 is desired for downstream MTBE synthesis and higher values usually are obtained, which is detrimental. The catalysts used in this study result in values of less than 1.0, and lower values can more easily be adjusted upward. Surface characterization data reveal that the reductive pretreatment given to the catalysts before exposure to the reactant feedstream causes an enrichment of the surface layer in the alkali promotor necessary for HAS. Data obtained from the pretreated catalysts before and after aging under reaction conditions indicate that a layered structure exists which consists of an alkali-enriched layer at the surface covering a Pd-enriched layer which resides above a ZnO phase over the Zn/Cr spinel support material. The alkali layer is reduced in size during aging in the reactor, although no significant changes in the product stream composition were noted over a 5-day test period. Differences are observed between the Cs-promoted and K-promoted catalysts which relate to why the Cs-promoted catalysts perform better.

ACKNOWLEDGMENTS

Financial support for this research was provided by the National Science Foundation through Grant CTS-9122575 and the Department of Energy through Contract DE-AC22-91PC90046.

REFERENCES

1. Klier, K., Beretta, A., Sun, Q., Feeley, O. C., and Herman, R. G., *Catal. Today* **36**, 3 (1997).
2. Forzatti, P., Tronconi, E., and Pasquon, I., *Catal. Rev.-Sci. Eng.* **33**, 109 (1991).
3. Apesteguia, C. R., DeRites, B., Miseo, S., and Soled, S., *Catal. Lett.* **44**, 1 (1997).
4. Xu, M., Gines, M. J. L., Hilmen, A.-M., Stephens, B. L., and Iglesia, E., *J. Catal.* **171**, 130 (1997).
5. Epling, W. S., Hoflund, G. B., and Minahan, D. M., *J. Catal.* **169**, 438 (1997).
6. Epling, W. S., Hoflund, G. B., and Minahan, D. M., *J. Catal.* **172**, 13 (1997).
7. Hoflund, G. B., Epling, W. S., and Minahan, D. M., *Catal. Lett.* **45**, 135 (1997).
8. Minahan, D. M., Epling, W. S., and Hoflund, G. B., *Appl. Catal. A* **166**, 375 (1997).
9. Epling, W. S., Hoflund, G. B., and Minahan, D. M., *J. Catal.* **175**, 175 (1998).
10. Simard, F., Sedran, U. A., Sepulveda, J., Figoli, N. S., and deLasa, H. I., *Appl. Catal.* **125**, 81 (1995).
11. Keim, W., and Falter, W., *Catal. Lett.* **3**, 59 (1989).
12. Vedage, G. A., Himelfarb, P. B., Simmons, G. W., and Klier, K., *Amer. Chem. Soc. Symp. Ser.* **279**, 295 (1985).
13. Beretta, A., Tronconi, E., Forzatti, P., Pasquon, I., Michell, E., Tagliabue, L., and Antoneli, G. B., *Ind. Eng. Chem. Res.* **35**, 2144 (1996).
14. Tronconi, E., Ferlazzo, N., Forzatti, P., and Pasquon, I., *Ind. Eng. Chem. Res.* **26**, 2122 (1987).
15. Boz, I., Sahibzada, M., and Metcalfe, I. S., *Ind. Eng. Chem. Res.* **33**, 2021 (1994).
16. Lietti, L., Tronconi, E., and Forzatti, P., *J. Catal.* **135**, 400 (1992).
17. Calverley, E. M., and Smith, K. J., *J. Catal.* **130**, 616 (1991).
18. Tronconi, E., Forzatti, P., and Pasquon, I., *J. Catal.* **124**, 376 (1990).
19. Nunan, J. G., Bogdan, C. E., Klier, K., Smith, K. J., Young, C.-W., and Herman, R. G., *J. Catal.* **116**, 195 (1989).
20. Nunan, J. G., Herman, R. G., and Klier, K., *J. Catal.* **116**, 222 (1989).
21. Stiles, A. B., Chen, F., Harrison, J. B., Hu, X., Storm, D. A., and Yang, H. X., *Ind. Eng. Chem. Res.* **30**, 811 (1991).
22. Campos-Martin, J. M., Fierro, J. L. G., Guerrero-Ruiz, A., Herman, R. G., and Klier, K., *J. Catal.* **163**, 418 (1996).
23. Hoflund, G. B., Epling, W. S., and Minahan, D. M., to be published.
24. Wagner, C. D., Riggs, W. M., Davis, L. E., Moulder, J. F., and Muilenberg, G. E., “Handbook of X-ray Photoelecton Spectroscopy.” Perkin-Elmer, Eden Prarie, MN, 1979.
25. Battistoni, C., Dormann, J. L., Fiorani, D., Paparazzo, E., and Viticoli, S., *Sol. State Comm.* **39**, 581 (1981).
26. Campos-Martin, J. M., Fiero, J. L. G., Guerrero-Ruiz, A., Herman, R. G., and Klier, K., *J. Catal.* **163**, 418 (1996).
27. Epling, W. S., Hoflund, G. B., and Minahan, D. M., *Surf. Sci. Spect.* **4**, 161 (1997).
28. Epling, W. S., Hoflund, G. B., and Minahan, D. M., *Surf. Sci. Spect.* **4**, 168 (1997).
29. Hoflund, G. B., *in* “Handbook of Surface and Interface Analysis: Methods in Problem Solving” (J. C. Rivière and S. Myhra, Eds.), p. 57. Dekker, New York, 1998.